



Deuteron beam fluence emitted from dense plasma focus: Comparative investigation and simulation

A. Altarabulsi^a • Y. Abou-Ali^{a*} • S. Alsheikh Salo^b • M. Akel^b • S. Lee^{c,d,e,f}

^aDepartment of Physics, Faculty of Science, University of Damascus, P.O. Box 30621, Damascus, Syria

^bDepartment of Physics, Atomic Energy Commission, Damascus, P.O. Box 6091, Syria

^cCentre for Plasma Research, INTI International University, 71800 Nilai, Malaysia

^dInstitute for Plasma Focus Studies, 32 Oakpark Drive, Chadstone 3148, Australia

^ePhysics Department, University of Malaya, Kuala Lumpur, Malaysia

^fFuse Energy Technologies, Napierville QC J0J 1L0, Canada

Received 01 14 2024; accepted 04 26 2024

Available 08 31 2024

Abstract: The fluence of a deuteron beam emitted from three dense plasma focus (DPF) devices, PF-1000, MPEF-12 kJ and PF-2.7 kJ, versus deuterium gas pressure was simulated and studied using the adapted Lee model code (RADPFV6.16FIB). The computed fluences were then compared to the reported measured values of these devices at certain distances from the pinch, where the comparison showed good agreement including within the range of errors. Furthermore, many numerical experiments using the Lee code were conducted and discussed for other different energy devices over a wide initial D₂ pressure range of (1 – 15 Torr), for studying the deuteron beam features at the pinch exit and various distances from the pinch. The obtained results indicated that the deuteron beam fluence is in order of 10²⁰ ions.m⁻² at the pinch exit for all the considered plasma focus devices (with energy storage included in the 0.2 – 863 kJ range) and this order can be reduced up to 10¹⁹ ions.m⁻² at the distance of 14 cm from the pinch exit. Therefore, the placement of treated material samples, using plasma focus, at different distances from the anode tip plays an essential role (in addition to the number of plasma shots) for multi-applications (e.g., ion implantation, thin film deposition and surface modification).

Keywords: Dense plasma focus, Lee model code, deuterons, ion beam, deuterons fluence, properties of deuterons, deuterium gas

*Corresponding author.

E-mail address: y.abouali@damascusuniversity.edu.sy (Y. Abou-Ali).

Peer Review under the responsibility of Universidad Nacional Autónoma de México.

1. Introduction

Dense plasma focus (DPF) devices are pulsed sources of neutrons (Marciniak et al., 2018; Wahbe et al., 2023), electron beams (Akel et al., 2018; Kubes et al., 2019), soft x-ray radiation (SXR) (Ay 2021; Barati 2023) and ion beams (Damideh et al., 2017; Etminan & Aghamir 2021; Ito et al., 2011; Kelly et al., 1998; Lee & Saw 2012b; 2013; Pestehe et al., 2014; Roshan et al., 2022). A column of pinched plasma in a DPF device is believed to typically produce pulsed ions from several of 100 keV to several of MeV (considering ions emitted from the nuclear fusion reactions) (Bertalot et al., 1980; Kubes et al., 2021; Malinowska et al., 2008; Mohanty et al., 2007; Mozer et al., 1982; Sadowski et al., 1988). Ion energies in DPF devices depend on the capacitors' bank energy, applied voltage, pinch current, gas type, gas pressure, materials used for manufacturing electrodes and insulators, and their geometry. Several researchers studied the properties of ion beams experimentally (Bertalot et al., 1980; Damideh et al., 2017; Etminan & Aghamir 2021; Ito et al., 2011; Kelly et al., 1998; Mozer et al., 1982; Pestehe et al., 2014) and numerically (Akel et al., 2017; Gribkov et al., 2007; Lee, 2014; Lee & Saw, 2012b) using the Lee model code as a useful tool for computing ion energy, density, flux, fluence, and plasma stream specifications (Lee & Saw, 2012b; 2013) due to its importance in several applications.

Space- and time-resolved investigation of high-energy deuterons emitted from three DPF devices was conducted (Sadowski et al., 1985). Ion beams were investigated using the Faraday Cup (FC) as a diagnostic tool for ion current density alongside ion time-of-flight (ToF) measurements (Damideh et al., 2017; Etminan & Aghamir 2021; Ito et al., 2011; Kelly et al., 1998; Pestehe et al., 2014). The ion energies are in the tens to hundreds of keV range, the pulse durations are tens of ns, and the currents are typically tens of kA (Gribkov et al., 2007). Fast deuterons of energies of about 100 keV (Kubes et al., 2021) and protons with energies of about 3 MeV (Malinowska et al., 2008), were studied using pinhole cameras equipped with solid-state nuclear track detectors (SSNTD).

Numerically, using the Lee model code, fast ions were studied to compute ion beam numbers, fluence and energy of fluence for numerous devices (Lee, 2014; Lee & Saw, 2012b). The measured ion current density, ion number density, ion energy and flux energy were found to match well with the computed values obtained using the Lee model code (Akel et al., 2017; Hassan et al. 2007; Mohanty et al., 2007). Published experimental data using time-resolved Schlieren imaging in the PF-400 J DPF device (Soto et al., 2014) were compared with the code results for post-focus pinch fast plasma stream (FPS) speeds and Stream Energy, power flow density, and damage factor. All computed quantities were found consistent with the measured quantities (Akel et al., 2016).

In several articles, the ion beams for various working gases were studied experimentally and numerically (Akel et al., 2016; 2022; Damideh et al., 2019). Extensive and systematic measurements were conducted using the FC, PIN diode detectors, and photomultiplier-scintillator measurements to study ion beams emitted from DPF devices operated with deuterium, neon and argon gases, and to correlate the measured results with results obtained using the Lee model code, thus providing conclusive experimental validation of the ion beam computations using the Lee model code (Akel et al., 2016; 2022; Damideh et al., 2019). In addition, the effect of the atomic number influence on the properties of the ion beams with three different working gases (He, N₂, Ar) was studied experimentally and numerically using the Lee model code (Akel et al., 2022).

The objective of this research is to investigate the fluence of deuterons emitted from the PF-1000 (863.1 kJ), MPEF-12 (9.7 kJ) and PF-2.7 kJ DPF devices using the Lee model code, and further evaluate its consistency in simulating the realistic values of ionic radiations emitted from the focused plasma which is produced in DPF devices. Furthermore, it aims to provide benchmark references of DPF devices to expert researchers in material processing using plasma focus technology.

2. Lee model code and ion beams emitted from DPF machines

The Lee model code (Lee, 2014; n.d.) couples the electric circuit parameters with the thermodynamic, dynamic, and radiation of plasma focus (PF). This code was initially implemented in 1983 (Lee & Saw, 2012b) and has been used for designing Mather-type DPF devices (Lee et al., 1988; Moo et al., 1991). The code was improved to be five-phase by adding a small finite disturbance speed (Lee, n.d.; Potter 1971). The version including radiation and radiation-coupled dynamics was introduced (Lee et al., 1998; Liu et al., 1998; Serban & Lee, 1997) and published in 2000 (Lee, 2014). In 2007, plasma self-absorption was included (Lee, 2014). The code has been widely used as a complementary tool for the simulation of discharges in numerous devices such as UNU-ICTP (Lee et al., 1988; 1998; Moo et al., 1991; Serban & Lee, 1997), NX1 (Lee et al., 1998), NX2 (Lee et al., 1998; Wong et al., 2006), and DENA DPF Filippov-type devices (Siahpoush et al., 2005). These studies provided diagnostic reference data for discharges in different gases. The main information obtained from the code includes the axial and radial dynamics of the current sheath (Abdou et al., 2012; Lee et al., 1988; Moo et al., 1991; Serban & Lee, 1997), SXR emission and its yield (Lee et al., 1998; Liu et al., 1998; Wong et al., 2006) and total neutron emission yield (Lee, 2009; Lee et al., 2009; Saw & Lee, 2010). The code was used to design DPF devices (Lee et al., 1988; 1998; Lee & Saw,

2012b; Liu et al., 1998; Serban & Lee, 1997), optimize DPF devices (Lee n.d.; Lee et al., 1988), develop Filippov-type DENA DPF devices (Siahpoush et al., 2005), determine current and neutron yield limitation (Lee & Saw, 2008b; Saw et al., 2009), investigate neutron saturation effect (Lee, 2009), investigate radiative collapse in plasma focus (Lee et al., 2013), develop current step technique to enhance plasma focus (Lee & Saw, 2012a) and obtain anomalous resistance data (Lee et al., 2011; Lee, 2014). The model was also improved and used to study ion beams emitted from DPF devices (Lee & Saw, 2012b; 2013).

To estimate the flux of the ion beam, (Lee & Saw, 2013) expressed the ion beam flux (ions. m⁻². s⁻¹) as:

$$J_b = n_b v_b \quad (1)$$

Here, n_b is the number of the beam ions (N_b) per unit of pinch volume (V_{pinch}), and v_b is the effective speed of the beam ions. The pinch volume can be expressed as $V_{pinch} = \pi r_{min}^2 z_p$, where r_{min} is the radius of the plasma pinch column and z_p is the effective length of the plasma column. Using the principle of energy conservation, (Lee & Saw, 2013) derived the J_b from the ion beam kinetic energy (BKE) and the pinch inductive energy (PIE). For an ion beam, which has N_b ions, where each ion has a mass Mm_p and effective speed v_b , the BKE relation can be written as follows:

$$BKE = \frac{1}{2} N_b M m_p v_b^2 \quad (2)$$

Where m_p is the proton mass, and M is the ion mass number. Moreover, BKE constitutes a portion f_e of PIE: $BKE = f_e PIE$, where $PIE = \frac{1}{2} L_p I_{pinch}^2$, therefore, BKE can be expressed with the following equation:

$$BKE = f_e PIE = \frac{1}{2} f_e L_p I_{pinch}^2 \quad (3)$$

Where L_p is the inductance of the plasma pinch, and I_{pinch} is the electric current flowing through the pinch taken at the beginning of the slow compression phase. The inductance of plasma pinch is expressed with $L_p = \frac{\mu}{2\pi} \ln\left(\frac{b}{r_{min}}\right) z_p$ relation, where $\mu = 4\pi \times 10^{-7} \text{H.m}^{-1}$ and b is the radius of the cathode (outer electrode). Using the above equations, the following relation is obtained (Lee & Saw, 2013).

$$Flux \text{ (ions. m}^{-2} \cdot \text{s}^{-1}) = J_b = 2.75 \times 10^{15} \frac{f_e}{(MZ_{eff})^{0.5}} \frac{\ln(b/r_{min})}{r_{min}^2} \frac{I_{pinch}^2}{U^{0.5}} \quad (4)$$

In the above equation, Z_{eff} is the effective ion charge and U is the plasma diode voltage. Hence, the fluence is the flux multiplied by the ion pulse duration τ (approximated using computed equilibrium pinch lifetime).

$$\begin{aligned} Fluence \text{ (ions. m}^{-2}) &= J_b \tau \\ &= 2.75 \\ &\times 10^{15} \frac{f_e}{(MZ_{eff})^{0.5}} \frac{\ln\left(\frac{b}{r_{min}}\right)}{r_{min}^2} \frac{I_{pinch}^2}{U^{0.5}} \tau \end{aligned} \quad (5)$$

The value of $f_e = 0.14$ (a portion of PIE which is converted into BKE) is equivalent to an ion beam energy of 3% – 6% E_0 (stored energy) in cases when the PIE has energy 20% – 40% E_0 as observed for low inductance DPF devices (Lee et al., 2011).

Based on the calculated flux, the other physical quantities of the ion beam can be written as follows (Lee & Saw, 2013).

- Energy flux (W. m^{-2}) = $J_b \times eZ_{eff}U$ (where U is the plasma diode voltage equal to $3V_{max}$ (Lee & Saw, 2012b.; Lee & Saw, 2008a; 2008b), and V_{max} is the maximum induced voltage of the radially collapsing current sheath (Lee & Saw, 2013) .
- Power flow (W) = Energy flux $\times \pi r_{min}^2$ (where πr_{min}^2 is the pinch cross-section).
- Ion current density (A. m^{-2}) = $J_b \times eZ_{eff}$ (eZ_{eff} is the effective ion charge).
- Ion beams current (A) = $J_b \times eZ_{eff} \times \pi r_{min}^2$.
- Ions per second (ions. s^{-1}) = $J_b \times \pi r_{min}^2$.
- Energy fluence (J. m^{-2}) = $J_b \times \tau \times eZ_{eff}U$.
- Number of ions in the beam (ions) = $J_b \times \tau \times \pi r_{min}^2$.
- Energy in beam (J) = number of ions in a beam $\times eZ_{eff}U = J_b \times \tau \times \pi r_{min}^2 \times eZ_{eff}U$.
- Damage factor ($\text{W. m}^{-2} \cdot \text{s}^{0.5}$) = $J_b \times eZ_{eff}U \times \tau^{0.5}$, where the damage factor is defined as the product of power flow density with the square root of plasma pinch lifetime (pinch duration) (Akel et al., 2016).

3. Fitting procedures using the Lee model code

Many numerical experiments have been conducted for the three reported DPF devices (PF-1000 (863.1 kJ) (Mateus et al., 2023), MEPF-12 kJ (9.7 kJ) (Niranjan et al., 2018) and PF-2.7 kJ (Lee & Saw, 2010) operated with deuterium filling gas using the Lee model code (RADPFV6.16FIB). Table 1 presents the parameters of these studied plasma focus devices.

Table 1. The electrical, geometric, gas and Lee model parameters of the PF-1000 kJ, MEPF-12 kJ and PF-2.7 kJ DPF devices. Where L_0 is the inductance of the device; C_0 is the total capacity of the capacitor bank; r_0 is the ohmic resistance of the device; b is the reduced radius of the cathode; a is the radius of the anode; z_0 is the effective length of the anode inside the experimental chamber; f_m , f_c , f_{mr} and f_{cr} are the Lee model parameters; V_0 is the charging voltage of the battery; p_0 is the initial working gas pressure; and M , Z and n are parameters describing the type of working gas.

Parameters	DPF devices		
	PF-1000	MPEF-12 kJ	PF-2.7 kJ
L_0 (nH)	33.5	65	110
C_0 (μ F)	1332	40	30
r_0 (m Ω)	6.3	1	22
b (cm)	16	5.5	3.2
a (cm)	11.5	3	0.95
z_0 (cm)	60	11.5	22
f_m	0.142	0.09	0.8
f_c	0.7	0.7	0.8
f_{mr}	0.2	0.1	0.5
f_{cr}	0.6	0.8	0.8
V_0 (kV)	36	22	13.5
p_0 (Torr)	3.5	3	0.15
M	4	4	4
Z	1	1	1
n	2	2	2

The MEPF-12 kJ DPF device was chosen to present full details of the simulation fitting procedures. First, the Lee model spreadsheet code was configured to work as virtual DPF devices by inserting the geometric and electrical parameters of the devices, as well as the parameters describing the used working gases (shown in Table 1). After setting up the spreadsheet (input file) of the code, a computed waveform current that simulates the DPF device has been obtained, but unreliably. Therefore, the computed discharge waveform current was fitted to the measured discharge waveform current by varying the Lee model parameters values

until a good agreement (fit) in the important parts of the two waveforms is obtained (Figure 1). The Lee model parameters are the mass (f_m , f_{mr}) and current factors (f_c , f_{cr}) of the axial and radial phases, respectively (Akel et al., 2012; Lee, 2014), considering all the phenomena in DPF which affect the mass and current distribution and attune for possible losses (Lee, 2014). During the fitting procedure, the change of L_0 (inductance of a DPF device) and r_0 (ohmic resistance of a DPF device) parameters may also be required. Figure 1 shows the final fit of the measured discharge current waveform with the (adjusted) computed discharge current waveform for the MEPF-12 kJ device using the parameters shown in Table 1.

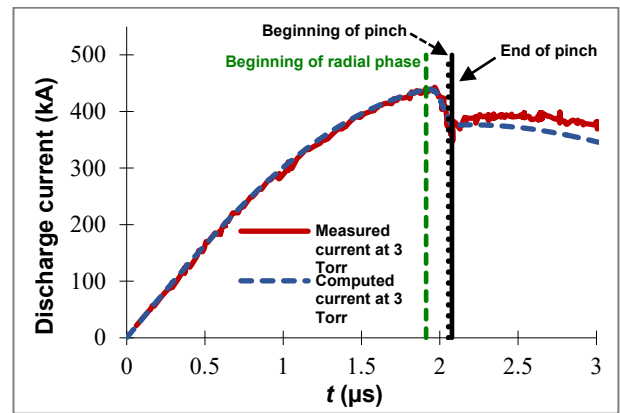


Figure 1. The measured (solid line) and computed (dashed line) current waveform of the MEPF-12 kJ DPF device operated with 3 Torr of initial deuterium pressure.

Figure 1 shows a good fitting agreement between the computed waveform current (dashed line) to the measured waveform current (solid line) for all the important parts of these two curves. It should be pointed out here that the fitting procedures were done up to the end of the pinch phase (at $\approx 2.08 \mu s$). Beyond this point, the divergence is insignificant and was not considered in the model (Lee & Saw, 2010). The non-importance of that phase after the end of the radial phase (end of a pinch) is attributed to the expected lack of further significant ion beam acceleration.

In general, the results of many previous studies suggested that the current trace of a plasma focus discharge is one of the best indicators of gross performance. The axial and radial phase dynamics and the crucial energy transfer into the plasma pinch are vital information in the current trace. The bank parameters, focus tube geometry and operational parameters govern the exact profile of the total current trace. It also depends on the fraction of mass swept up and the fraction of sheath current and should also be sensitive to the variation of these fractions through the axial and radial phases. These parameters determine the axial and radial dynamics, specifically the axial and radial speeds that affect the profile and magnitudes of the discharge current. The

detailed profile of the discharge current also reflects the Joule heating and radiative yields during the pinch phase. At the end of the pinch phase, the total current profile also reflects the sudden transition of the current flow from a constricted pinch to a large column flow (plasma expansion). Thus, the discharge current powers all dynamic, electrodynamic, thermodynamic and radiation processes in the various phases of the plasma focus. Also, all the dynamics, electrodynamic, thermodynamic and radiation processes in the various phases of the plasma focus, conversely, affect the discharge current. Then, it is no exaggeration to say that the discharge current waveform contains information on all the dynamics, electrodynamic, thermodynamic and radiation processes that occur in the various phases of the plasma focus. This explains the importance of matching the computed current trace to the measured current trace in the procedure adopted by the Lee model code. Once the waveform currents are fitted, the code should be able to output the following data realistically (approximately): Dynamics and energy content of the phases, plasma column geometry, temperatures and densities, line radiation, neutron yields, ion beam properties, fast plasma stream dynamics and energies.

Employing the same methodology, the presented procedure for matching (fitting) the total discharge waveform currents (and their importance) has been applied in the same manner to all the plasma focus devices considered in this work.

4. Results and discussions

4.1. Comparison with experimental data

In much previous research, the Lee model code has been evaluated as a simulator code for DPF devices. For instance, the measured power flow density of deuteron beams emitted from the PF-400 J DPF device was compared to the Lee model computations with good agreement (Akel et al., 2016). Moreover, the behavior of the simulated ion beam current density versus the initial pressure of the nitrogen gas was discussed and well compared with the observed measurements (Akel et al., 2017). Besides, the ion beam flux and fluence computed by the Lee model were found to be in coincidence with the measured values (Damideh et al., 2017). These reasonable agreements between the computations of the Lee model code and some of the measured ion beam features provided the authors with more confidence to continue conducting numerical experiments. Then, comparing available measured deuteron beam properties with those computations, reliably, i.e., with the measured deuteron fluence emitted from the PF-1000, MEPF-12 kJ and PF-2.7 kJ DPF devices. It is worth mentioning that the obtained data of the Lee model for the ion beam is computed at the pinch exit ($R = 0$). Table 2 shows the computed deuteron fluence at the pinch exit using the Lee model code for the

PF1000, MEPF-12 kJ and PF-2.7 kJ devices. One can notice that the deuteron fluence increases with higher initial D₂ pressure and can reach a value of an order of 10^{20} ions. m⁻² for all the studied devices.

Table 2. The computed fluence of deuterons emitted from PF-1000, MEPF-12 kJ and PF2.7 kJ DPF using the Lee model code at the pinch exit $R = 0$.

PF-1000	
p_0 (Torr)	Fluence (ions. m ⁻²) × 10 ¹⁹
0.2	4.7
0.3	6.4
0.4	7.9
0.5	9.3
0.6	10.7
0.7	12.0
MEPF-12 kJ	
p_0 (Torr)	Fluence (ions. m ⁻²) × 10 ¹⁹
0.76	5.9
1.49	9.7
2.24	13.0
3	16.1
4.5	21.6
6	26.4
7.5	30.8
PF-2.7 kJ	
p_0 (Torr)	Fluence (ions. m ⁻²) × 10 ¹⁹
0.075	3.0
0.15	4.8
0.225	6.7
0.375	9.8
0.6	14.1

In the DPF devices, the emitted beam will move with a conic-like form and at a distance from the pinch after leaving the pinch area. The interaction with the medium traversed and beam and stream divergence will attenuate the propagating ion beam. Therefore; to study the deuteron beam fluence at different distances from the pinch exit, the following additional computations are carried out using the formula (Sanchez & Feugeas, 1997): $f_i = \frac{N_i}{\sigma_R}$. In this formula, N_i is the ion beam (deuterons) number per shot taken from the Lee model code computations at the pinch exit, while $\sigma_R = \pi(R \cdot \tan\theta)^2$ is the cross-section of the ion beam solid angle at a distance R from the pinch exit, and θ is the half angle. For these estimations, energy loss due to interaction with background gas is considered negligible. In Table 3, the computed results of deuteron fluence at a distance from the pinch are compared with the reported measured values for the PF-1000, MPEF-12 kJ and PF-2.7 kJ versus gas pressure (experimental results were already published and discussed in (Lim et al., 2018; Mateus et al., 2023; Niranjana et al., 2018)). To understand the physical and chemical processes of the ion interaction with the surface, reliable information on ion fluence and flux for different plasma focus devices versus pressures must be obtained. Table 3 shows the evaluation of the measured fluence of deuterons emitted from the PF-1000, MPEF-12 kJ and PF-2.7 kJ, and computed fluences at different distances from the plasma pinch.

In Table 3, one can notice that the deuteron fluence decreases from an order of 10^{20} ions. m^{-2} at the pinch exit to 10^{19} (for PF-1000 at 14 cm), 10^{18} (for MPEF-12 kJ at 14 cm) and 10^{15} (for PF-2.7 kJ at 40 cm). The computed and measured beam fluences are in good agreement for the three studied devices. From Table 3 one can also find out that fluence increases with higher pressures for PF-1000 and MPEF-12 kJ, while for PF-2.7 kJ the fluence peaks at the pressure of 0.15 Torr. The fluence behavior is attributed to the plasma focus efficiency which requires optimum initial gas pressure at which the maximum pinch current intensity and highest transferred energy into the plasma are obtained.

4.2. Numerical simulations for different energy DPF devices

In this section, since the Lee model code computations of the previous section are validated. Simulations for nine different energy DPF devices: PF-143 (20.2 kJ) (Yousefi et al., 2006), PF-24 (16.8 kJ) (Marciniak et al., 2018), BARC (11.5 kJ) (Niranjana, 2017), Hanyang (4.1 kJ) (Woo et al., 2004), PF-12 (2.6

kJ) (Laas et al. 2020), DPF-2.2 (2.2 kJ) (Wang et al., 1999), Montecucolino (2.3 kJ) (Frignani, 2007), ISPF (200 J) (Niranjana et al., 2011), Nanofocus (100 J) (Milanese et al., 2003) were conducted to provide the experts with benchmark values of the most important ion beam properties, where all computations and fitting procedures were repeated and followed systemically the same methodologies for the studied DPF devices. The deuteron fluences at the pinch exit $R = 0$ were computed and summarized in Table 4. Presented data in Table 4 show that the fluences at the pinch exit are of an order of 10^{20} ions. m^{-2} for all devices. The deuteron fluence at 14 cm from the pinch exit for all devices was also computed and summarized in Table 5. Tables 4 and 5 indicate that the fluence values also have the same order of 10^{20} ions. m^{-2} at $R = 0$ and 10^{19} ions. m^{-2} at $R = 14$ cm for different energy devices. The computed results could be useful for material science applications using a small DPF machine instead of employing expensive facilities. Since the fluence is computed, the other properties for materials science application could be obtained. For instance, the deuteron flux was included in the range of $10^{25} - 10^{27}$ ions. $m^{-2} \cdot s^{-1}$ for all the DPF devices. The energy of flux ranges from 10^{10} W. m^{-2} for the Nanofocus device to 10^{14} W. m^{-2} for the PF-143 device, whereas the damage factor values range from 10^7 W. $m^{-2} \cdot s^{0.5}$ to 10^9 W. $m^{-2} \cdot s^{0.5}$. It is worth mentioning that there are three typical modes of influence of ion beam upon a target material placed downstream of the pinch (Akel et al., 2017; Gribkov et al., 2007): (1) “implantation mode” of irradiation when the power flow density of the streams is ($10^9 - 10^{11}$ W. m^{-2}), (2) “detachment mode” where screening of the surface by a secondary plasma cloud takes place ($10^{11} - 10^{12}$ W. m^{-2}), and (3) “explosive destruction mode” where strong damage takes place with the absence of implantation ($10^{12} - 10^{14}$ W. m^{-2}). So, based on the computed energy flux for all DPF devices, it can be said that the small low-energy plasma focus devices are more suitable for ion implantation, while the higher energy is for detachment and explosive modes.

To study the effect of distances R from the pinch exit on the deuterons fluence, many numerical experiments have been conducted on the PF-24 kJ device. Figure 2 illustrates the deuteron fluence of the PF-24 kJ device in terms of distances R from the pinch exit (where the fluence is 3.87×10^{20} ions. m^{-2}) at a gas pressure of 11 Torr. It shows that the beam fluence reduces with distance from the pinch due to the divergence of the ion beam up to 1.16×10^{19} ions. m^{-2} (at 26 cm).

Table 3. Comparisons of the experimental deuteron fluence, emitted from PF-1000, MEPF-12 kJ and PF-2.7 kJ DPF devices to the computed fluence using the Lee model code at a distance $R = 14\text{ cm}$, 14 cm and 40 cm , respectively, from the pinch exit as they were measured, (both current waveforms for each device were fitted at $p_0 = 3.5\text{ Torr}$, 3 Torr and 0.15 Torr , respectively). The (–) symbol indicates that there are no experimental results to compare with.

PF-1000 at $R = 14\text{ cm}$		
p_0 (Torr)	Fluence (Sim.) (ions.m ⁻²) × 10 ¹⁹	Fluence (Exp.) (ions.m ⁻²) × 10 ¹⁹
0.2	3.7	-
0.3	5.0	-
0.4	6.2	-
0.5	7.3	~ 7.5
0.6	8.4	-
0.7	9.4	-

MEPF-12 kJ at $R = 14\text{ cm}$		
p_0 (Torr)	Fluence (Sim.) (ions.m ⁻²) × 10 ¹⁸	Fluence (Exp.) (ions.m ⁻²) × 10 ¹⁸
0.76	5.5	5.57 ± 0.84
1.49	5.9	5.79 ± 0.81
2.24	6.5	6.53 ± 0.78
3	7.5	7.05 ± 0.7
4.5	6.8	6.68 ± 0.82
6	5.6	5.75 ± 0.81
7.5	6.0	6.15 ± 0.94

PF-2.7 kJ at $R = 40\text{ cm}$		
p_0 (Torr)	Fluence (Sim.) (ions.m ⁻²) × 10 ¹⁵	Fluence (Exp.) (ions.m ⁻²) × 10 ¹⁵
0.075	3.99	3.89 ± 0.48
0.15	4.94	4.95 ± 0.25
0.225	4.14	4.06 ± 0.21
0.375	3.68	3.77 ± 0.16
0.6	1.77	1.86 ± 0.11

Table 4. The Lee model code computations for the deuteron fluence initial D₂ pressure for the studied devices at the pinch exit $R = 0$. The (–) symbol indicates that computations were stopped due to the Lee code limits.

p_0 (Torr)	Fluence (ions. m ⁻²) × 10 ²⁰								
	PF-143	PF-24	BARC	Hanyang	PF-12	DPF-2.2	Monte Cucolino	ISPF	Nanofocus
1.0	1.5	0.7	1.4	1.0	1.1	0.7	0.7	0.4	0.5
3.0	3.3	1.5	3.0	2.3	2.4	1.6	1.4	0.9	0.9
5.0	4.7	2.2	4.3	3.4	3.6	2.3	1.6	1.3	0.8
7.0	5.7	2.9	5.3	4.3	4.5	3.0	-	1.6	-
9.0	6.3	3.4	6.0	5.7	5.5	3.6	-	1.9	-
11.0	5.9	3.9	6.5	6.3	6.3	4.2	-	2.2	-
13.0	4.1	4.3	6.6	6.4	7.0	4.7	-	2.4	-
15.0	-	-	6.2	5.8	7.7	5.2	-	2.5	-

Table 5. Computed fluence versus initial D₂ pressure using the Lee model code for all studied devices at a distance $R = 14$ cm from the pinch exit. The (–) symbol indicates that computations were stopped due to the Lee code limits.

Fluence (ions. m ⁻²) × 10 ¹⁹									
P_0 (Torr)	PF-143	PF-24	BARC	Hanyang	PF-12	DPF-2.2	Monte Cucolino	ISPF	Nanofocus
1.0	1.20	1.01	1.46	2.88	2.08	1.06	0.97	0.15	0.34
3.0	2.03	1.89	2.72	5.42	4.81	2.39	1.89	0.26	0.48
5.0	2.90	2.67	3.81	6.77	6.33	2.91	1.46	2.27	0.30
7.0	3.67	3.31	4.73	7.71	8.11	4.55	-	8.84	-
9.0	3.83	3.85	4.75	6.12	6.98	3.54	-	7.45	-
11.0	3.00	4.00	3.44	2.68	6.04	3.07	-	4.89	-
13.0	1.33	1.16	2.38	1.60	3.44	1.75	-	4.43	-
15.0	-	-	1.00	1.00	1.74	1.26	-	3.64	-

Figure 2. The fluence variation over distances R from the pinch exit at a gas pressure of 11 Torr where the calculated flux is the highest.

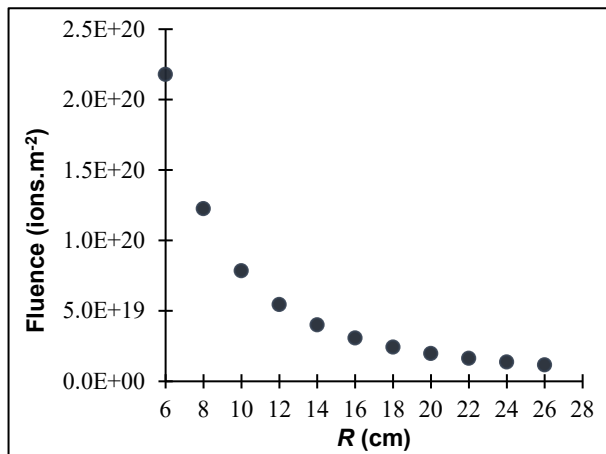


Figure 2 (for the PF-24 device) shows computations for other computed ion beam properties such as flux, energy flux and damage factor. The flux ranges from 8.7×10^{27} ions. m⁻². s⁻¹ at the pinch exit to 2.61×10^{26} ions. m⁻². s⁻¹ at 26 cm distance; while the energy of flux is reduced from 1.37×10^{14} W. m⁻² at the pinch exit to 4.09×10^{12} W. m⁻² at 26 cm distance. The deuteron damage factor is decreased over the same distance from 2.88×10^{10} W. m⁻². s^{0.5} to 8.63×10^8 W. m⁻². s^{0.5}.

5. Summary and conclusion

Investigation of the fluence of deuterons emitted from the PF-1000, MPEF-12 kJ and PF-2.7 kJ DPF devices in terms of initial D₂ pressure was conducted using the Lee model code, including, a comparison of the measured and computed val-

ues of fluence for these devices was conducted. The comparison of measured and computations of the MPEF-12 kJ and PF-2.7 kJ DPF devices showed the same behavior of the investigated quantities with good agreement including the range of errors, where the deuteron fluence increases as the pressure increases until it reaches the maximum, then it reduces when the pressure goes further. For the PF-1000, only one deuteron fluence value was detected and registered at (0.5 Torr), where the computed deuteron fluence using the Lee model code was 7.3×10^{19} ions. m⁻² which is close to the measured fluence that equals to about $\sim 7.5 \times 10^{19}$ ions. m⁻².

Moreover, a deuteron fluence simulation using the Lee model code of the nine different energy DPF devices versus initial D₂ pressure has been conducted. The obtained computed values were investigated at a constant distance $R = 14$ cm from the pinch exit and compared with the calculated fluence values at the pinch exit $R = 0$. In addition, the deuteron fluence as a function of distance R for the PF-24 DPF device was chosen, computed, and studied at a fixed initial D₂ pressure (11 Torr) at which the deuteron flux is the highest. The carried partial study shows that the fluence decreases with increasing distance far from the pinch exit point. The presented noteworthy results from this article could be used as benchmark references in different applications and fields including plasma processing such as ion implantation, surface modification, thermal surface treatment, ion-assisted coating, device fabrication, and thin film deposition.

Conflict of interest

The author(s) has (have) no conflict of interest to declare.

Acknowledgements

The authors would like to thank Damascus University, The Ministry of Higher Education of the Syrian Arab Republic, and the General Director of the AECS for encouragement and permanent support.

Financing

The authors did not receive any sponsorship to conduct the research reported in the present manuscript.

References

Abdou, A. E., Ismail, M. I., Mohamed, A. E., Lee, S., Saw, S. H., & Verma, R. (2012). Preliminary results of Kansas State University dense plasma focus. *IEEE Transactions on Plasma Science*, 40(10), 2741-2744.

<https://doi.org/10.1109/TPS.2012.2209682>

Akel, M., AL-Hawat, S., Ahmad, M., Ballul, Y., & Shaaban, S. (2022). Features of Pinch Plasma, Electron, and Ion Beams That Originated in the AECS PF-1 Plasma Focus Device. *Plasma*, 5(2), 184-195.

<https://doi.org/10.3390/plasma5020014>

Akel, M., Al-Hawat, S., Lee, S., & Saw, S. H. (2018). Characterization of electron beams emitted from dense plasma focus machines using argon, neon and nitrogen. *Modern Physics Letters B*, 32(32), 1850397.

<https://doi.org/10.1142/S0217984918503979>

Akel, M., Alsheikh Salo, S., Ismael, S., Saw, S. H., & Lee, S. (2016). Deuterium plasma focus as a tool for testing materials of plasma facing walls in thermonuclear fusion reactors. *Journal of Fusion Energy*, 35, 694-701.

<https://doi.org/10.1007/s10894-016-0092-z>

Akel, M., Salo, S. A., Ismael, S., Saw, S. H., & Lee, S. (2017). Comparison of measured and computed beam ion current densities emitted from two 2 kJ plasma focus machines. *Vacuum*, 136, 163-167.

<https://doi.org/10.1016/j.vacuum.2016.12.005>

Akel, M., Lee, S., & Saw, S. H. (2012). Numerical experiments in plasma focus operated in various gases. *IEEE Transactions on Plasma Science*, 40(12), 3290-3297.

<https://doi.org/10.1109/TPS.2012.2220863>

Ay, Y. (2021). Neon soft x-ray yield optimization in spherical plasma focus device. *Plasma Physics and Controlled Fusion*, 63(11), 115009.

<https://doi.org/10.1088/1361-6587/ac206d>

Barati, H. (2023). Investigation of nitrogen soft X-ray emission from dense plasma focus with anode with curved tip using the lee model. *Journal of Fusion Energy*, 42(1), 1.

<https://doi.org/10.1007/s10894-022-00339-3>

Bertalot, L., Herold, H., Jäger, U., Mozer, A., Oppenländer, T., Sadowski, M., & Schmidt, H. (1980). Mass and energy analysis and space-resolved measurements of ions from plasma focus devices. *Physics Letters A*, 79(5-6), 389-392.

[https://doi.org/10.1016/0375-9601\(80\)90272-8](https://doi.org/10.1016/0375-9601(80)90272-8)

Damideh, V., Ali, J., Saw, S. H., Rawat, R. S., Lee, P., Chaudhary, K. T., ... & Sing, L. (2017). Fast Faraday cup for fast ion beam TOF measurements in deuterium filled plasma focus device and correlation with Lee model. *Physics of Plasmas*, 24(6).

<https://doi.org/10.1063/1.4985309>

Damideh, V., Chin, O. H., Saw, S. H., Lee, P. C. K., Rawat, R. S., & Lee, S. (2019). Characteristics of Fast ion beam in Neon and Argon filled plasma focus correlated with Lee Model Code. *Vacuum*, 169, 108916.

<https://doi.org/10.1016/j.vacuum.2019.108916>

Etminan, M., & Aghamir, F. M. (2021). Angular distribution of ion beams energy and flux in a plasma focus device operated with argon gas. *Vacuum*, 191, 110352.

<https://doi.org/10.1016/j.vacuum.2021.110352>

Frignani, M. (2007). *Simulation of gas breakdown and plasma dynamics in plasma focus devices*.

Gribkov, V. A., Bienkowska, B., Borowiecki, M., Dubrovsky, A. V., Ivanova-Stanik, I., Karpinski, L., ... & Tomaszewski, K. (2007). Plasma dynamics in PF-1000 device under full-scale energy storage: I. Pinch dynamics, shock-wave diffraction, and inertial electrode. *Journal of Physics D: Applied Physics*, 40(7), 1977.

<https://doi.org/10.1088/0022-3727/40/7/021>

Hassan, M., Qayyum, A., Ahmad, R., Murtaza, G., & Zakauallah, M. (2007). Nitriding of titanium by using an ion beam delivered by a plasma focus. *Journal of Physics D: Applied Physics*, 40(3), 769.

<https://doi.org/10.1088/0022-3727/40/3/013>

- Ito, H., Nishino, Y., & Masugata, K. (2011). Emission characteristics of a high-energy pulsed-ion-beam produced in a dense plasma focus device. *Journal of the Korean Physical Society*, 59(61), 3674-3678.
<https://doi.org/10.3938/jkps.59.3674>
- Kelly, H., Lepone, A., Marquez, A., Sadowski, M. J., Baranowski, J., & Skladnik-Sadowska, E. (1998). Analysis of the nitrogen ion beam generated in a low-energy plasma focus device by a Faraday cup operating in the secondary electron emission mode. *IEEE transactions on plasma science*, 26(1), 113-117.
<https://doi.org/10.1109/27.659540>
- Kubes, P., Paduch, M., Sadowski, M. J., Cikhardt, J., Cikhardtova, B., Klir, D., ... & Akel, M. (2021). Characteristics of fast deuteron sources generated in a dense plasma focus. *The European Physical Journal Plus*, 136(8), 810.
<https://doi.org/10.1140/epjp/s13360-021-01799-w>
- Kubes, P., Paduch, M., Sadowski, M. J., Cikhardt, J., Cikhardtova, B., Klir, D., ... & Zielinska, E. (2019). Evolution of a pinch column during the acceleration of fast electrons and deuterons in a plasma-focus discharge. *IEEE Transactions on Plasma Science*, 47(1), 339-345.
<https://doi.org/10.1109/TPS.2018.2874288>
- Laas, T., Laas, K., Paju, J., Priimets, J., Tökke, S., Väli, B., ... & Akel, M. (2020). Behaviour of tungsten alloy with iron and nickel under repeated high temperature plasma pulses. *Fusion Engineering and Design*, 151, 111408.
<https://doi.org/10.1016/j.fusengdes.2019.111408>
- Lee, S. (2009). Neutron yield saturation in plasma focus: A fundamental cause. *Applied Physics Letters*, 95(15).
<https://doi.org/10.1063/1.3246159>
- Lee, S. (n.d.) Institute for Plasma Focus Studies.
<http://www.plasmafocus.net/IPFS/modelpackage/File1RADPF.htm>
- Lee, S. (2014). Plasma focus radiative model: Review of the Lee model code. *Journal of Fusion Energy*, 33, 319-335.
<https://doi.org/10.1007/s10894-014-9683-8>
- Lee, S., Lee, P., Zhang, G., Feng, X., Gribkov, V. A., Liu, M., ... & Wong, T. K. (1998). High rep rate high performance plasma focus as a powerful radiation source. *IEEE Transactions on Plasma Science*, 26(4), 1119-1126.
<https://doi.org/10.1109/27.725141>
- Liu, M. (1996). Soft X-rays from compact plasma focus (Doctoral dissertation). <http://hdl.handle.net/10356/20374>
- Lee, S., & Saw, S. H. (2008a). Neutron scaling laws from numerical experiments. *Journal of Fusion Energy*, 27, 292-295.
<https://doi.org/10.1007/s10894-008-9132-7>
- Lee, S., & Saw, S. H. (2008b). Pinch current limitation effect in plasma focus. *Applied Physics Letters*, 92(2).
<https://doi.org/10.1063/1.2827579>
- Lee, S., & Saw, S. H. (2010). A course on plasma focus numerical experiments. In *Joint ICTP-IAEA Workshop on Dense Magnetized Plasmas and Plasma Diagnostics*.
- Lee, S., & Saw, S. H. (2012a). Current-step technique to enhance plasma focus compression and neutron yield. *Journal of fusion energy*, 31, 603-610.
<https://doi.org/10.1007/s10894-012-9506-8>
- Lee, S., & Saw, S. H. (2012b). Plasma focus ion beam fluence and flux—Scaling with stored energy. *Physics of Plasmas*, 19(11).
<https://doi.org/10.1063/1.4766744>
- Lee, S., & Saw, S. H. (2013). Plasma focus ion beam fluence and flux—For various gases. *Physics of Plasmas*, 20(6).
<https://doi.org/10.1063/1.4811650>
- Lee, S., Saw, S. H., Abdou, A. E., & Torreblanca, H. (2011). Characterizing plasma focus devices—Role of the static inductance—Instability phase fitted by anomalous resistances. *Journal of fusion energy*, 30, 277-282.
<https://doi.org/10.1007/s10894-010-9372-1>
- Lee, S., Saw, S. H., & Ali, J. (2013). Numerical experiments on radiative cooling and collapse in plasma focus operated in krypton. *Journal of Fusion Energy*, 32, 42-49.
<https://doi.org/10.1007/s10894-012-9522-8>
- Lee, S., Saw, S. H., Soto, L., Springham, S. V., & Moo, S. P. (2009). Numerical experiments on plasma focus neutron yield versus pressure compared with laboratory experiments. *Plasma Physics and Controlled Fusion*, 51(7), 075006.
<https://doi.org/10.1088/0741-3335/51/7/075006>
- Lee, S., Tou, T. Y., Moo, S. P., Eissa, M. A., Gholap, A. V., Kwek, K. H., ... & Zakaullah, M. (1988). A simple facility for the teaching of plasma dynamics and plasma nuclear fusion. *American Journal of Physics*, 56(1), 62-68.
<https://doi.org/10.1119/1.15433>

- Lim, L. K., Yap, S. L., & Bradley, D. A. (2018). Time-resolved characteristics of deuteron-beam generated by plasma focus discharge. *Plos one*, 13(1), e0188009. <https://doi.org/10.1371/journal.pone.0188009>
- Liu, M., Feng, X., Springham, S. V., & Lee, S. (1998). Soft X-ray yield measurement in a small plasma focus operated in neon. *IEEE Transactions on Plasma Science*, 26(2), 135-140. <https://doi.org/10.1109/27.669614>
- Malinowska, A., Malinowski, K., Sadowski, M. J., Zebrowski, J., & Szydłowski, A. (2008). Experimental studies of fast protons originated from fusion reactions in plasma-focus discharges. In *AIP Conference Proceedings* (Vol. 993, No. 1, pp. 353-356). American Institute of Physics. <https://doi.org/10.1063/1.2909146>
- Marciniak, Ł., Akel, M., Kulińska, A., Scholz, M., Lee, S., Kunze, H. J., & Saw, S. H. (2018). Measurements and simulations of neutron emission versus deuterium filling pressure in plasma focus device PF-24. *Journal of Fusion Energy*, 37(2), 124-129. <https://doi.org/10.1007/s10894-018-0157-2>
- Mateus, R., Czarkowski, P., Martins, R., Vitor, C. M., Dias, M., Malaquias, A., ... & Alves, E. (2023). Ion beam analysis of W irradiated with deuterium-based plasma discharges at PF-1000U. *Nuclear Instruments and Methods in Physics Research Section B: Beam Interactions with Materials and Atoms*, 541, 279-285. <https://doi.org/10.1016/j.nimb.2023.05.067>
- Milanese, M., Moroso, R., & Pouzo, J. (2003). DD neutron yield in the 125 J dense plasma focus nanofocus. *The European Physical Journal D-Atomic, Molecular, Optical and Plasma Physics*, 27, 77-81. <https://doi.org/10.1140/epjd/e2003-00247-9>
- Mohanty, S. R., Neog, N. K., Bhuyan, H., Rout, R. K., Rawat, R. S., & Lee, P. (2007). Effect of anode designs on ion emission characteristics of a plasma focus device. *Japanese journal of applied physics*, 46(5R), 3039. <https://doi.org/10.1143/JJAP.46.3039>
- Moo, S. P., Chakrabarty, C. K., & Lee, S. (1991). An investigation of the ion beam of a plasma focus using a metal obstacle and deuterated target. *IEEE transactions on plasma science*, 19(3), 515-519. <https://doi.org/10.1109/27.87231>
- Mozer, A., Sadowski, M., Herold, H., & Schmidt, H. (1982). Experimental studies of fast deuterons, impurity-and admixture-ions emitted from a plasma focus. *Journal of Applied Physics*, 53(4), 2959-2964. <https://doi.org/10.1063/1.331033>
- Niranjan, R. (2017). Ion Emission Study of Plasma Focus devices and its applications in material science. [Thesis]. <http://hdl.handle.net/10603/308732>
- Niranjan, R., Rout, R. K., Mishra, P., Srivastava, R., Rawool, A., Kaushik, T. C., & Gupta, S. C. (2011). Note: A portable pulsed neutron source based on the smallest sealed-type plasma focus device. *Review of scientific instruments*, 82(2). <https://doi.org/10.1063/1.3534827>
- Niranjan, R., Rout, R. K., Srivastava, R., & Kaushik, T. C. (2018). Effect of gas filling pressure and operation energy on ion and neutron emission in a medium energy plasma focus device. *Journal of Applied Physics*, 123(9). <https://doi.org/10.1063/1.4993990>
- Pestehe, S. J., Mohammadnejad, M., & Irani Mobaraki, S. (2014). Dynamic Faraday cup signal analysis and the measurement of energetic ions emitted by plasma focus. *Physics of Plasmas*, 21(3). <https://doi.org/10.1063/1.4867175>
- Potter, D. E. (1971). Numerical studies of the plasma focus. *The Physics of Fluids*, 14(9), 1911-1924. <https://doi.org/10.1063/1.1693700>
- Roshan, M. V., Roshan, N. V., & Yap, S. L. (2022). High energy ion beams from the plasma focus. *Applied Radiation and Isotopes*, 185, 110224. <https://doi.org/10.1016/j.apradiso.2022.110224>
- Sadowski, M., Rydygier, E., Herold, H., Jäger, U., & Schmidt, H. (1985). Multi-spike structure of ion pulses generated by plasma focus discharges. *Physics Letters A*, 113(1), 25-31. [https://doi.org/10.1016/0375-9601\(85\)90599-7](https://doi.org/10.1016/0375-9601(85)90599-7)
- Sadowski, M., Zebrowski, J., Rydygier, E., & Kucinski, J. (1988). Ion emission from plasma-focus facilities. *Plasma physics and controlled fusion*, 30(6), 763. <https://doi.org/10.1088/0741-3335/30/6/008>
- Sanchez, G., & Feugeas, J. (1997). The thermal evolution of targets under plasma focus pulsed ion implantation. *Journal of Physics D: Applied Physics*, 30(6), 927. <https://doi.org/10.1088/0022-3727/30/6/004>

- Saw, S. H., Lee, P. C. K., Rawat, R. S., & Lee, S. (2009). Optimizing UNU/ICTP PFF plasma focus for neon soft X-ray operation. *IEEE Transactions on Plasma Science*, 37(7), 1276-1282.
<https://doi.org/10.1109/TPS.2009.2022167>
- Saw, S. H., & Lee, S. (2010). Scaling laws for plasma focus machines from numerical experiments. *Energy and Power Engineering*, 2(01), 65.
- Serban, A., & Lee, S. (1997). Soft X-ray emission from a small plasma focus operated in deuterium. *Plasma Sources Science and Technology*, 6(1), 78.
<https://doi.org/10.1088/0963-0252/6/1/011>
- Siahpoush, V., Tafreshi, M. A., Sobhanian, S., & Khorram, S. (2005). Adaptation of Sing Lee's model to the Filippov type plasma focus geometry. *Plasma physics and controlled fusion*, 47(7), 1065.
<https://doi.org/10.1088/0741-3335/47/7/007>
- Soto, L., Pavez, C., Moreno, J., Inestrosa-Izurietta, M. J., Veloso, F., Gutiérrez, G., ... & Delgado-Aparicio, L. F. (2014). Characterization of the axial plasma shock in a table top plasma focus after the pinch and its possible application to testing materials for fusion reactors. *Physics of Plasmas*, 21(12).
<https://doi.org/10.1063/1.4903471>
- Wahbe, S., Abou-Ali, Y., Akel, M., Lee, S., & Marciniak, L. (2023). Numerical experiments on the total D-D fusion neutron yield versus deuterium pressure for different energy plasma focus devices using the Lee model code. *Plasma Physics and Controlled Fusion*, 65(5), 055022.
<https://doi.org/10.1088/1361-6587/acc610>
- Wang, X., Han, M., Wang, Z., & Liu, K. (1999). A compact plasma focus device and its neutron emission. *Science in China Series E: Technological Sciences*, 42(1), 83-87.
<https://doi.org/10.1007/BF02917062>
- Wong, D., Lee, P., Zhang, T., Patran, A., Tan, T. L., Rawat, R. S., & Lee, S. (2006). An improved radiative plasma focus model calibrated for neon-filled NX2 using a tapered anode. *Plasma Sources Science and Technology*, 16(1), 116.
<https://doi.org/10.1088/0963-0252/16/1/016>
- Woo, H. J., Chung, K. S., & Lee, M. J. (2004). Dependence of neutron yield on the deuterium filling pressure in a plasma focus device. *Plasma physics and controlled fusion*, 46(7), 1095.
<https://doi.org/10.1088/0741-3335/46/7/009>
- Yousefi, H. R., Mohanty, S. R., Nakada, Y., Ito, H., & Masugata, K. (2006). Compression and neutron and ion beams emission mechanisms within a plasma focus device. *Physics of plasmas*, 13(11).
<https://doi.org/10.1063/1.2388961>